

# A Simple Graphical-Based Proportional–Integral–Derivative Tuning Method for Time-Delay Systems

Gülten Çetintaş<sup>1</sup>, Münevver Mine Özyetkin<sup>2</sup>, Serdar Ethem Hamamcı<sup>3</sup>

<sup>1</sup>Department of Electrical Electronics Engineering, Muş Alparslan University, Muş, Turkey

<sup>2</sup>Department of Electrical Electronics Engineering, Aydın Adnan Menderes University, Aydın, Turkey

<sup>3</sup>Department of Electrical Electronics Engineering, İnönü University, Malatya, Turkey

**Cite this article as:** G. Çetintaş, M. Mine Özyetkin and S. Ethem Hamamcı, "A simple graphical-based proportional–integral–derivative tuning method for time-delay systems," *Electrica*, 23(2), 376-384, 2023.

## ABSTRACT

In this paper, a graphical-based proportional–integral–derivative (PID) tuning technique for time-delay systems is presented. The suggested tuning technique combines the stability boundary locus (SBL) method with the weighted geometrical center (WGC) concept. The plot of the stability region obtained by using real root boundary (RRB), infinite root boundary (IRB), and complex root boundary (CRB) in the parameter plane forms the basis of the proposed method. The tuning steps of the method can be expressed as follows. First, the stability region in  $(k_d, k_p)$ -plane is obtained using the SBL for the fixed RRB line. Thus, the stability value range of the  $k_d$  parameter is determined. Second, using these  $k_d$  values, the entire set of stability regions in  $(k_p, k_i)$ -plane is obtained. These regions constitute a three-dimensional global stability region in  $(k_p, k_i, k_d)$  space. Finally, the WGC points of stability regions in each  $(k_p, k_i)$ -plane are calculated. The center point having the best time domain performance among these WGC points is determined. This point gives the PID tuning parameters for the proposed method. The simulation results indicate that the presented tuning technique gives simple and reliable results and is useful in the stability analysis and the control of time-delay systems.

**Index Terms**—PID tuning, stabilization, time delay, weighted geometrical center

## I. INTRODUCTION

In the real world, time delay is a common type of behavior encountered in system dynamics. This phenomenon is an important problem to be considered in many physical, industrial, and engineering systems. The time delay has a notable and complex effect on the dynamics of the system, and this effect can adversely influence the time response of the system and may even lead to instability [1]. Recently, important studies have been carried out on the stability and control analysis of time-delay systems [2].

The proportional–integral–derivative (PID) control is one of the most preferred control techniques for time-delay systems by control system designers because its control system structure is simple and the number of controller parameters to be considered for the tuning process is only three [3]. Many tuning methods for the PID controllers have been developed for industrial purposes [4]. In order to obtain satisfactory control performance, various methods such as fuzzy logic-based tuning [5], linear programming technique [6], transient response control method [7], IMC (Internal Model Control)-based method [8], genetic algorithm-based method [9] have been reported in the last few decades. These studies can be basically classified under three categories as time domain methods, frequency domain methods, or optimal control methods.

The concept of obtaining the stability region in the parameter space of PI and PID controller parameters has been one of the most studied topics for nearly 30 years. There are many studies on the PI and PID stabilization in the literature, for example, Hermite–Biehler Theorem [10], stability boundary locus (SBL) method [11], parameter space method [12, 13], D-Decomposition method [14, 15]. However, these methods give only stability region which includes all stabilizing controller parameters. On the other hand, some valuable studies are reported on which the controller parameter values can give a better time response than the other values in the obtained stability region. FTDP (Frequency and Time Domain Performances)-map method has been proposed in [16] that provides the desired frequency and time domain properties in the stability

### Corresponding author:

Gülten Çetintaş

### E-mail:

gultencetintas@gmail.com

**Received:** August 9, 2022

**Accepted:** January 3, 2023

**Publication Date:** March 30, 2023

**DOI:** 10.5152/electr.2022.22147



Content of this journal is licensed under a Creative Commons Attribution-NonCommercial 4.0 International License.

region. The centroid stable point method has been proposed for only a class of second-order systems in [17].

Recently, a new PI tuning method for the time-delay systems has been proposed using the weighted geometrical center (WGC) method, also known as Onat's method, which uses the stability region graphically [18, 19]. The WGC method is based on the calculation of the WGC of the region of stabilizing controller parameters and has been used successfully in many studies [18–22]. However, these studies have only been reported for PI- and PD-based controllers. In this study, the WGC method has been extended to PID control of the time-delay systems. Although some preliminary results for WGC-based tuning of PID controllers have been published in [23], the optimality is not considered in this paper. However, in our paper, the WGC point which gives the best time response for the control system is obtained in the three-dimensional stability region.

In this paper, a simple and efficient PID tuning technique based on the WGC method is presented for the time-delay systems. In this technique, first, the PID stability region is obtained with the SBL method, and then optimal PID tuning is performed using the WGC method for the PID controller. One of the most important advantages of the method is that it works for a wide range of time-delay systems such as stable, unstable, and integrator systems. In addition, the proposed method has some important advantages in terms of calculating the controller parameters without using complex graphical methods and quickly determining the optimum controller parameter values inside the global stability region that results in good unit step response for time-delayed systems.

## II. PRELIMINARIES

### A. Proportional–Integral–Derivative Control System

The PID control system is a unit feedback control system consisting of a plant and a PID controller to control the plant. Consider a general PID control system shown in Fig. 1, in which  $r(t)$  is the reference input,  $e(t)$  is the error signal,  $u(t)$  is the control signal, and  $y(t)$  is the output signal. The plant shown in the figure is a time-delay system and is defined by the transfer function given as

$$G(s) = \frac{N(s)}{D(s)} e^{-\tau s} \quad (1)$$

where  $N(s)$  and  $D(s)$  are the numerator and denominator polynomials of the plant transfer function, respectively, and  $\tau$  is the time delay. The PID controller in Fig. 1 is in parallel structure and has the transfer function formulated as follows.

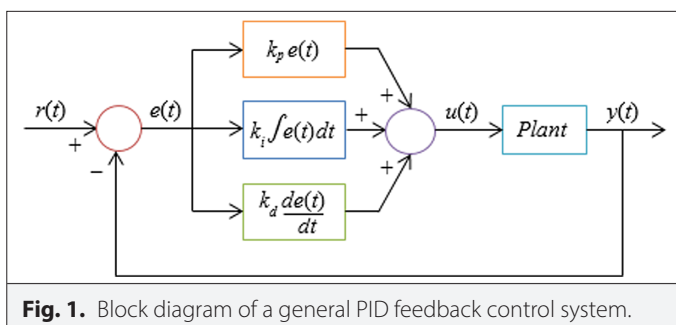


Fig. 1. Block diagram of a general PID feedback control system.

$$C(s) = k_p + \frac{k_i}{s} + k_d s \quad (2)$$

where  $k_p$ ,  $k_i$ , and  $k_d$  denote the proportional, integral, and derivative gains, respectively. The characteristic equation of the control system is

$$P(s, k_p, k_i, k_d) = 1 + G(s)C(s) = sD(s) + (k_d s^2 + k_p s + k_i)N(s)e^{-\tau s}. \quad (3)$$

### B. Stability Boundary Locus Method

Conversion of the complex plane to the parameter space using the conformal mapping technique is one of the important techniques frequently used in control system design. In the SBL method, which is one of these techniques, the parameter space is divided into regions consisting of a fixed number of stable and unstable roots for a characteristic polynomial, and the stability region that makes the control system stable is obtained. It is a graphical method and is especially used for the stabilization of control systems containing PID-based controllers [11]. The most important tools of the SBL method are stability boundaries. These boundaries isolate the stability region from the instability regions.

In a characteristic polynomial, the roots pass from the left half plane to the right half plane in the complex plane in three different ways, according to the change of the controller parameters. They define three different types of stability boundaries listed below [12, 13, 24]:

- (1) Real Root Boundary (RRB): A root of the characteristic polynomial crosses the imaginary axis of the complex plane on the origin through the real axis. This corresponds to crossing a stability boundary obtained as  $P(s=0, k_p, k_i, k_d) = 0$  in the parameter space as a result of the mapping process. For the characteristic equation in (3), the RRB is obtained as

$$k_i = 0 \quad (4)$$

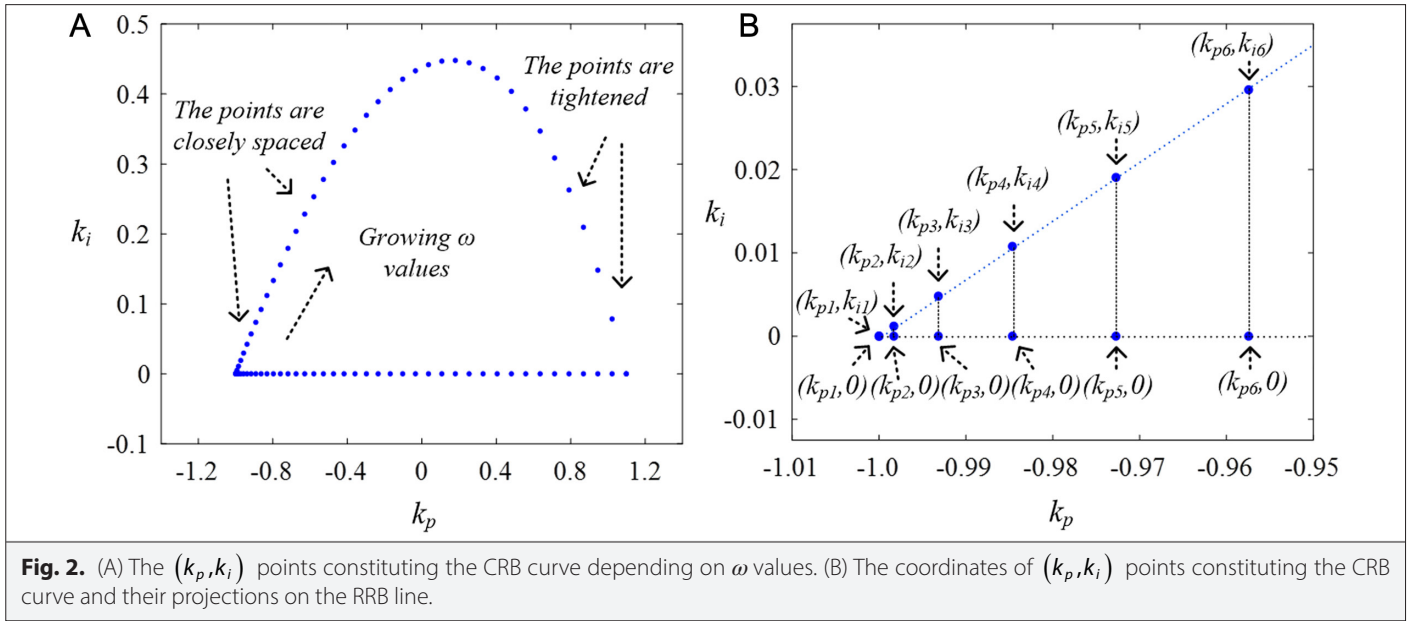
- (2) Infinite Root Boundary (IRB): A root of the characteristic polynomial leaves left or right half plane of the complex plane at infinity. This case matches up to crossing a stability boundary expressed as  $P(|s| \rightarrow \infty, k_p, k_i, k_d) = 0$  in the parameter space with the mapping. The IRB for the characteristic equation in (3) can be expressed as

$$IRB : \begin{cases} \text{none} & \deg\{D(s)\} \geq \deg\{N(s)\} + 2 \\ k_d = \pm d_m / n_m & \deg\{D(s)\} = \deg\{N(s)\} + 1 \\ k_d = 0 & \deg\{D(s)\} = \deg\{N(s)\} \end{cases} \quad (5)$$

where  $n_m$  and  $d_m$  are the coefficients of the largest order terms of the numerator and denominator polynomials, respectively.

- (3) Complex Root Boundary (CRB): A pair of complex roots of the characteristic polynomial crosses on the imaginary axis of the complex plane. This corresponds to crossing a stability boundary obtained as  $P(s = j\omega, k_p, k_i, k_d) = 0$  in the parameter space as a result of the mapping process. The CRB is obtained by solving the system of linear equations obtained by substituting  $j\omega$  for  $s$  in the characteristic equation in (3) and equating its real ( $P_R$ ) and imaginary ( $P_I$ ) parts to zero, as seen in the following equations:

$$P(\omega) = P_R(\omega) + jP_I(\omega) = 0 \quad (6)$$



where

$$P_R(\omega) = (-\omega^2 k_p N_o + k_i N_e - \omega^2 k_d N_e) \cos(\tau\omega) + \omega(k_p N_e + k_i N_o - \omega^2 k_d N_o) \sin(\tau\omega) - \omega^2 D_o \quad (7)$$

$$P_I(\omega) = \omega(k_p N_e + k_i N_o - \omega^2 k_d N_o) \cos(\tau\omega) + (\omega^2 k_p N_o - k_i N_e + \omega^2 k_d N_e) \sin(\tau\omega) + \omega D_e \quad (8)$$

$$G(\omega) = \frac{N_e(-\omega^2) + j\omega N_o(-\omega^2)}{D_e(-\omega^2) + j\omega D_o(-\omega^2)} e^{-j\omega\tau} \quad (9)$$

$$P_R(\omega) = 0 \Rightarrow k_p A(\omega) + k_i B(\omega) + k_d C(\omega) = X(\omega) \quad (10)$$

$$P_I(\omega) = 0 \Rightarrow k_p D(\omega) + k_i E(\omega) + k_d F(\omega) = Y(\omega) \quad (11)$$

where

$$A(\omega) = -\omega^2 N_o \cos(\tau\omega) + \omega N_e \sin(\tau\omega),$$

$$B(\omega) = N_e \cos(\tau\omega) + \omega N_o \sin(\tau\omega)$$

$$C(\omega) = -\omega^2 N_e \cos(\tau\omega) - \omega^3 N_o \sin(\tau\omega),$$

$$D(\omega) = \omega N_e \cos(\tau\omega) + \omega^2 N_o \sin(\tau\omega)$$

$$E(\omega) = \omega N_o \cos(\tau\omega) - N_e \sin(\tau\omega),$$

$$F(\omega) = -\omega^3 N_o \cos(\tau\omega) + \omega^2 N_e \sin(\tau\omega)$$

$$X(\omega) = \omega^2 D_o, Y(\omega) = -\omega D_e.$$

Finally, the three-variable system in (10) and (11) is converted to the two-variable systems, assuming one variable is constant, and a solution is made.

These stability boundaries drawn separately in  $(k_p, k_i, k_d)$ -space divide the whole space into sub-regions. For any sub-region, the characteristic polynomials formed by all  $(k_p, k_i, k_d)$  triplets in this

sub-region have the same number of stable and unstable poles. Each sub-region has its own unique feature in this way.

**Remark 2.1:** A sub-region is called a *stability region* if the characteristic polynomials formed by all  $(k_p, k_i, k_d)$  triplets in it always have stable poles. All sub-regions outside the stability region are called the *instability region*. Therefore, if a controller is to be selected for a system, it must be selected from within the stability region.

### C. Weighted Geometrical Center Method

The WGC method is an important and graphical method proposed for selecting the controller with the best time response among all stable PI controllers in the stability region obtained by using the SBL method for a system [19].

The WGC method is a technique developed based on the SBL method. The main theme of the method is to obtain the WGC point of the frequency points forming the stability boundaries. In the SBL method, the CRB curve forming the stability region is obtained by giving values to  $\omega$  in  $G(j\omega)$ . This curve simply consists of points in the  $(k_p, k_i)$ -plane whose coordinates are defined as  $(k_{p1}, k_{i1}), (k_{p2}, k_{i2}), \dots, (k_{pn}, k_{in})$  as seen in Fig. 2(a). Here  $n$  is the number of  $(k_{p2}, k_{i2})$  pairs that make up the CRB. The most important feature of these points on the curve is that the distances between them are not the same. As seen in the figure, while the points are more closely spaced at some  $\omega$  values, they diverge at some other  $\omega$  values. In addition, the RRB line, which is another stability boundary, is formed independently of the values of  $\omega$ . Therefore, in the WGC method, the projections of the points on the CRB are obtained to take into account the effect of the RRB line, as shown in Fig. 2(b). Considering the points on CRB and RRB together, the WGC point of the stability region is easily obtained as follows:

$$k_{p\omega} = \frac{1}{n} \sum_{j=1}^n k_{pj} \quad (12)$$

$$k_{i\omega} = \frac{1}{2n} \sum_{j=1}^n k_{ij} \quad (13)$$

where  $k_{p\omega}$  and  $k_{i\omega}$  correspond to the optimal PI parameters. Interested readers may refer to paper [11] for the SBL method and [18–22] for the WGC method.

### III. WEIGHTED GEOMETRICAL CENTER METHOD-BASED OPTIMAL PROPORTIONAL–INTEGRAL–DERIVATIVE TUNING PROCEDURE

In this section, a design procedure for PID tuning using the WGC method is presented. The proposed method basically consists of four steps. In the first step, the CRB curve is calculated by using (10) and (11) as follows:

$$k_p = \frac{(\omega^2 D_o N_o + D_e N_e) \cos(\tau\omega) + \omega(N_o D_e - N_e D_o) \sin(\tau\omega)}{-(N_e^2 + \omega^2 N_o^2)} \quad (14)$$

$$k_i = \frac{\begin{bmatrix} (\omega^4 N_o^2 D_o + \omega^2 N_o N_e D_e) \cos^2(\tau\omega) + \omega^2 (N_e^2 D_o - N_e N_o D_e) \sin^2(\tau\omega) \\ + (-2\omega^3 N_e N_o D_o + \omega^3 N_o^2 D_e - \omega N_e^2 D_e) \cos(\tau\omega) \sin(\tau\omega) \\ - k_d ((\omega^2 N_e^3 + \omega^4 N_e N_o^2) \cos(\tau\omega) + (\omega^3 N_e^2 N_o + \omega^5 N_o^3) \sin(\tau\omega)) \\ - \omega^2 (N_e^2 D_o + \omega^2 N_o^2 D_o) \end{bmatrix}}{\begin{bmatrix} (-N_e^3 - \omega^2 N_e N_o^2) \cos(\tau\omega) + (-\omega N_e^2 N_o - \omega^3 N_o^3) \sin(\tau\omega) \end{bmatrix}} \quad (15)$$

$$k_d = \frac{\begin{bmatrix} (\omega^4 N_o^2 D_o + \omega^2 N_o N_e D_e) \cos^2(\tau\omega) + \omega^2 (N_e^2 D_o - N_e N_o D_e) \sin^2(\tau\omega) \\ + (-2\omega^3 N_e N_o D_o + \omega^3 N_o^2 D_e - \omega N_e^2 D_e) \cos(\tau\omega) \sin(\tau\omega) \\ - k_i ((-N_e^3 - \omega^2 N_e N_o^2) \cos(\tau\omega) + (-\omega N_e^2 N_o - \omega^3 N_o^3) \sin(\tau\omega)) \\ - \omega^2 (N_e^2 D_o + \omega^2 N_o^2 D_o) \end{bmatrix}}{\begin{bmatrix} (\omega^2 N_e^3 + \omega^4 N_e N_o^2) \cos(\tau\omega) + (\omega^3 N_e^2 N_o + \omega^5 N_o^3) \sin(\tau\omega) \end{bmatrix}} \quad (16)$$

From (14)–(16), it is seen that  $k_i$  and  $k_d$  are dependent on each other and  $k_p$  is independent of these two parameters.

In the second step, the stability value range for the  $k_d$  parameter is determined by obtaining the two-dimensional stability region for  $k_i = 0$  value corresponding to the RRB in the  $(k_p, k_d)$  parameter plane. This value range plays a key role in the three-dimensional stability region in the next step. In this step, the CRB curve drawn in the  $(k_p, k_d)$  -plane is constrained by the  $k_p = -D(0)$  line because for the RRB value in (4), the controller turns to the PD controller and thus an auxiliary RRB arises. In the third step, for the stable values of  $k_d$ , two-dimensional stability regions are obtained in the  $(k_p, k_i)$  -plane. By plotting these regions together, a three-dimensional stability region is obtained in  $(k_p, k_i, k_d)$  -space. In the last step, the best  $(k_p, k_i, k_d)$  triples as the number of regions are obtained by using the WGC technique for the two-dimensional  $(k_p, k_i)$  stability regions obtained for each stable  $k_d$  value. These triplets give the best PID parameter value locally for the considered  $k_d$  values. Finally, these triplets are tested to obtain the best PID controller globally. Here, the

most important factor affecting the result is the step size used for  $k_d$  while obtaining the local best PID parameter triplets, and keeping the step size of  $k_d$  small provides a more precise result.

### IV. SIMULATION EXAMPLES

#### A. Example 1

Consider the transfer function of the first-order plus time-delay system has the form

$$G(s) = \frac{1}{s+1} e^{-s} \quad (17)$$

Here, the aim is to obtain the  $k_p$ ,  $k_i$ , and  $k_d$  parameters of the PID controller using the WGC method. The characteristic equation of the control system is determined as

$$\Delta(s) = s^2 + s + (k_p s + k_i + k_d s^2) e^{-s} \quad (18)$$

The RRB line is obtained as  $k_i = 0$  from (4) and the IRB line is found as  $k_d = \pm 1$  from (5). For the CRB curve, the following parameter equations are obtained:

$$k_p = \omega \sin \omega - \cos \omega \quad (19)$$

$$k_i = \omega^2 \cos \omega + \omega \sin \omega + \omega^2 k_d \quad (20)$$

$$k_d = (-\omega^2 \cos \omega - \omega \sin \omega + k_i) / \omega^2 \quad (21)$$

Figure 3 shows the stability boundaries  $(k_d, k_p)$ -plane for  $k_i = 0$ . The CRB line is constrained with  $k_p = -1$  line because for the value  $k_i = 0$ , the controller returns to the PD controller and in this case, an auxiliary RRB has arisen. As shown in Fig. 3, the parameter plane is divided into nine sub-regions, namely  $R_1, R_2, R_3, R_4, R_5, R_6, R_7, R_8$ , and  $R_9$ . If a test point is selected from each sub-region and the unit step responses of the control system for the test points are plotted, it is obtained that the  $R_2$  sub-region is the stable region. Therefore, considering the CRB and IRB limiting the  $R_2$  sub-region, it is determined that the stability value range of the  $k_d$  parameter is  $(-1, 1)$ . However,

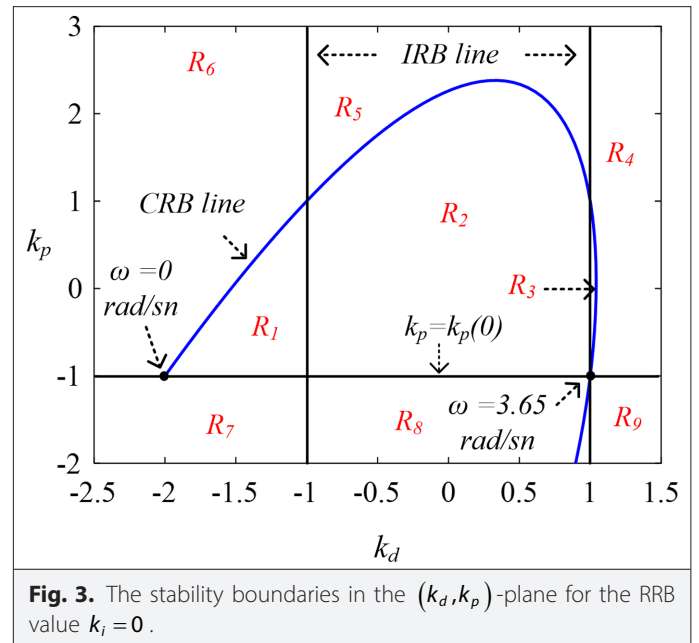


**Fig. 3.** The stability boundaries in the  $(k_d, k_p)$ -plane for the RRB value  $k_i = 0$ .

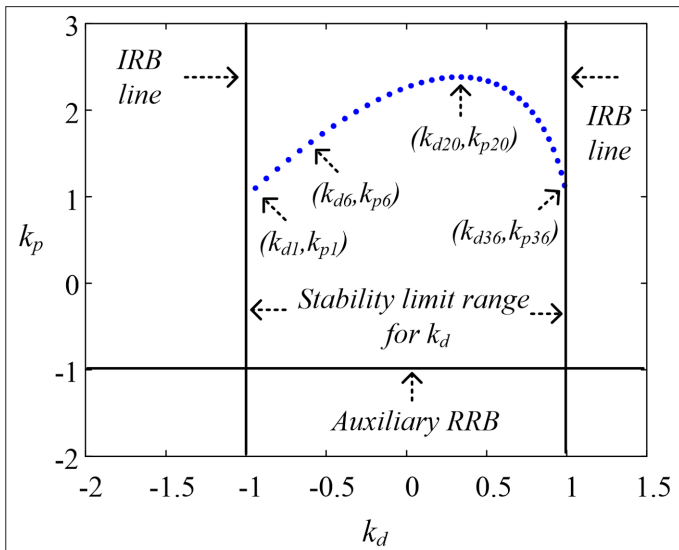


**Fig. 4.** The  $(k_d, k_p)$  points constituting the CRB curve in the parameter plane.

not all points in this range have equal stability. This is illustrated by the fact that the points in Fig. 4 that form the CRB curve in the  $R_2$  sub-region as a result of  $\omega$  changing from 1.35 rad/s to 3.1 rad/s in 0.05 intervals are not evenly spaced. The  $k_d$  values, which are 36 in total, are determined from this figure.

After determining the stability limit range for  $k_d$ , the stability regions are plotted in the  $(k_p, k_i)$ -plane for the 36  $k_d$  values determined earlier. For example, the stability boundaries for the initial value of  $k_d$ ,  $k_{d1} = -0.9418$ , are shown in Fig. 5. It can be observed from this figure that the parameter plane is divided into four sub-regions, namely  $R_1$ ,  $R_2$ ,  $R_3$ , and  $R_4$ . By choosing one arbitrary test point in each sub-region, the stability region which is the shaded sub-region  $R_1$  shown in Fig. 5 is determined. These 36 stability regions obtained in the  $(k_p, k_i)$ -plane form the global stability region in three-dimensional  $(k_p, k_i, k_d)$ -space as shown in Fig. 6.

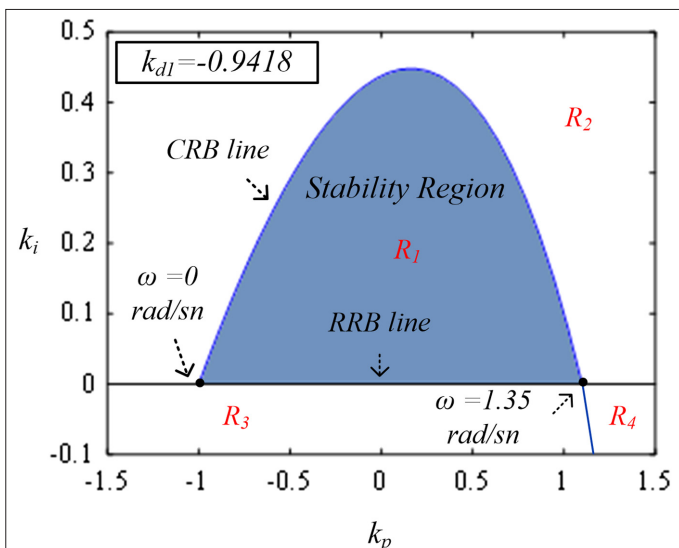


**Fig. 5.** For  $k_{d1} = -0.9418$ , (a) Stability boundaries. (b) Stability region in the  $(k_p, k_i)$ -plane.

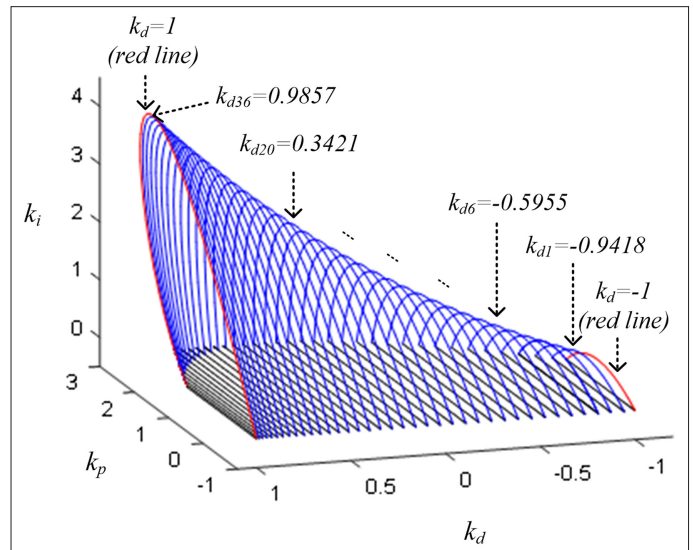


**Fig. 6.** The global stability region in three-dimensional  $(k_p, k_i, k_d)$ -space.

At this stage, the WGC point that gives a good transient response for the control system within the obtained three-dimensional stability region will be obtained. For this, the WGC points of the 36 two-dimensional stability regions obtained in the  $(k_p, k_i)$ -plane are determined as given in Section III. For example, for  $k_{d1} = -0.9418$ , the two-dimensional stability region obtained in the  $(k_p, k_i)$ -plane and its WGC point are shown in Fig. 7. This point is calculated as  $k_{pw} = -0.212$ ,  $k_{iw} = 0.118$ , and  $k_{dw} = -0.9418$ . The same operations are performed for the other  $k_d$  values, respectively.

Table I and Fig. 8(a) show the 4 WGC points and their unit step responses that give the best unit response among the 36  $k_d$  values. As can be seen from the figure, the best results are as follows.  $k_p = 0.4212$ ,  $k_i = 0.4370$  for  $k_d = -0.0385$  and  $k_p = 0.3757$ ,  $k_i = 0.4048$  for  $k_d = -0.1062$ . Here, the designer can take additional action to get a more accurate result. For this,  $k_{d14} = -0.0385$  and

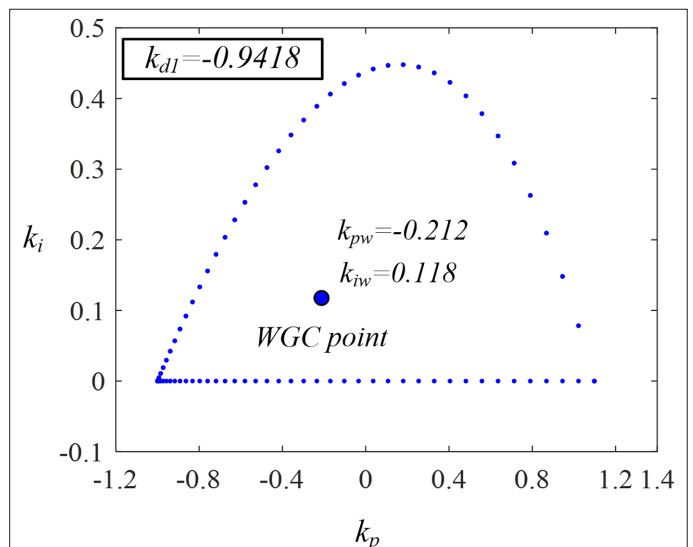


**Fig. 7.** The WGC point of stability region for  $k_{d1} = -0.9418$ .

**TABLE I.** FOUR WGC POINTS THAT GIVE THE BEST UNIT RESPONSE AMONG THE STABLE 36  $k_d$  VALUES

Point Number	$k_d$	$k_p$	$k_i$	Time Response Color in Fig. 8(a)
12	-0.1748	0.3292	0.3736	Blue
13	-0.1062	0.3757	0.4048	Red
14	-0.0385	0.4212	0.4370	Green
15	0.0282	0.4655	0.4703	Violet

WGC, weighted geometrical center.

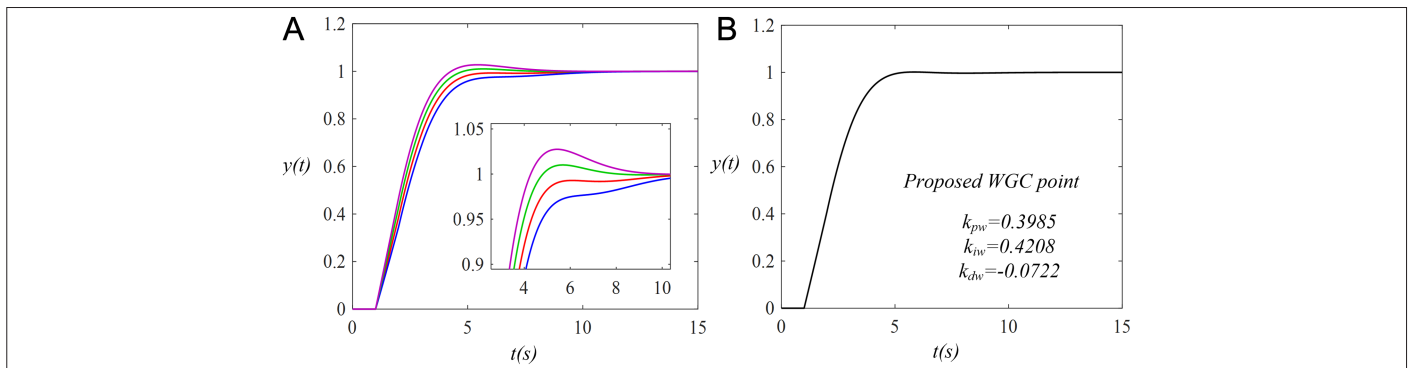


**Fig. 8.** (A) The step responses of the PID control systems for different WGC points (The color relations of the PID parameter values and the step responses are given in Table I). (B) Step response for  $k_{pw} = 0.3985$ ,  $k_{iw} = 0.4208$ , and  $k_{dw} = -0.0722$  obtained as the best PID tuning parameters.

$k_{d13} = -0.1062$ , which give the best two results, are divided into ten equal intervals and the same operations are repeated to obtain the best time response among them. A more precise result is obtained for  $k_{dw} = -0.0722$ ,  $k_{pw} = 0.3985$ , and  $k_{iw} = 0.4208$ . The closed-loop response for a unit step reference input is given in Fig. 8(b). In Fig. 9, the three-dimensional global stability region and the obtained WGC point are illustrated in the  $(k_p, k_i, k_d)$  parameter space.

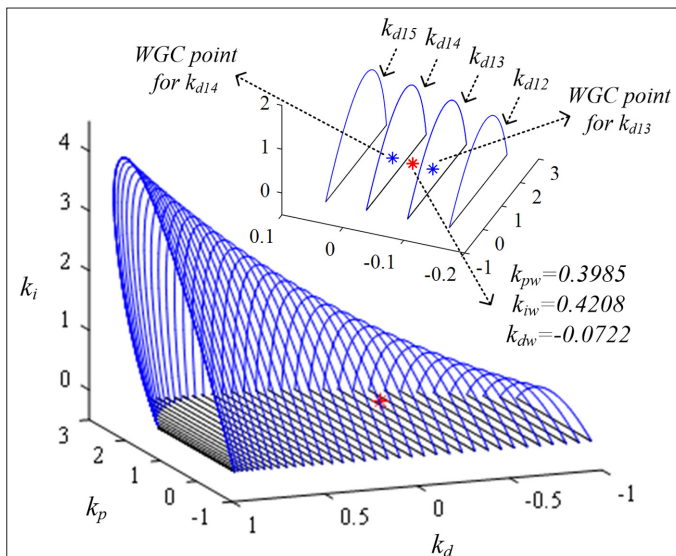


**Fig. 9.** Three-dimensional global stability region and the obtained WGC point in the  $(k_p, k_i, k_d)$  parameter space.

To show the goodness of the time response given by the obtained PID parameters, a comparison is made with the results of Toscano [25]. The PID parameters of Toscano's PID tuning method are  $k_p = 0.846$ ,  $k_i = 0.7007$ , and  $k_d = 0.2501$ . The closed-loop unit step responses of two tuning methods are shown in Fig. 10. It can be seen from the figure that the time response obtained with the proposed method is much better than that obtained by Toscano's method.

**B. Example 2**

Consider a second-order unstable system with time delay

$$G(s) = \frac{1}{(5s-1)(2s+1)(0.5s+1)} e^{-0.5s} \quad (22)$$

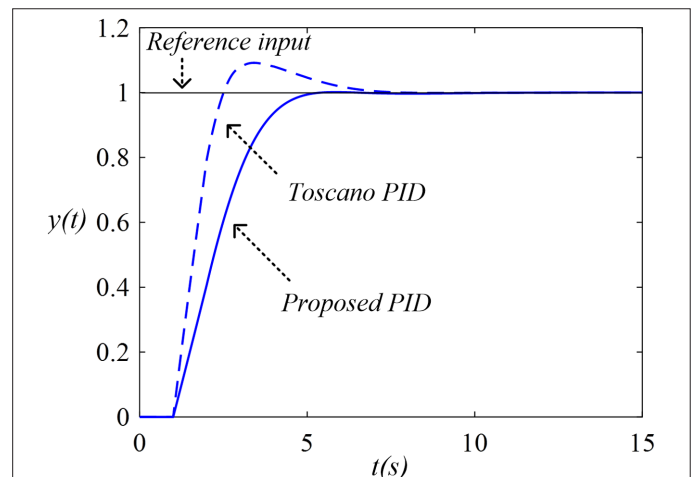


**Fig. 10.** Comparisons of the closed-loop unit step responses.

For this system, the RRB line is  $k_i = 0$  and there is no IRB line. By applying the procedure given in Section III, the three-dimensional global stability region and the calculated WGC point for this region are shown in Fig. 11. The PID tuning parameters for the proposed method are  $k_{pw} = 3.9193$ ,  $k_{iw} = 0.4286$ , and  $k_{dw} = 6.3809$ .

For comparison, the results for PID design methods proposed by Lee et al. [26], Huang and Chen [27], and Poulin and Pomerleau [28] are also given. The controller parameters are given by  $k_p = 7.144$ ,  $k_i = 0.069$ ,  $k_d = 11.823$ ;  $k_p = 6.186$ ,  $k_i = 0.863$ ,  $k_d = 9.106$ ; and  $k_p = 3.05$ ,  $k_i = 0.404$ ,  $k_d = 6.314$ , respectively. The response to a unit step input change for the proposed design and the design methods proposed by the others are illustrated in Fig. 12. This

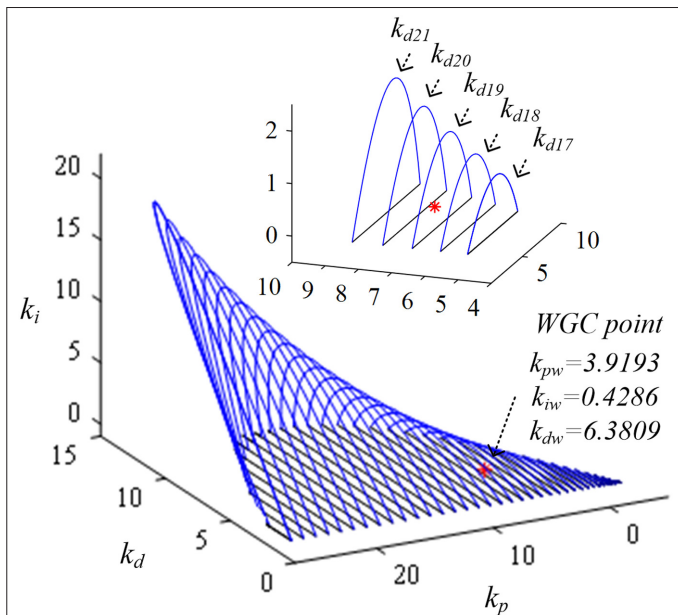


**Fig. 11.** The three-dimensional global stability region and its WGC point for the PID tuning.

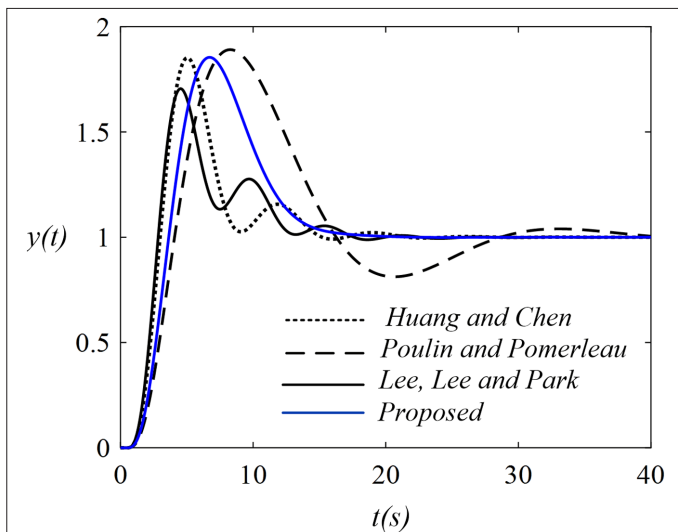


**Fig. 12.** Comparisons of the closed-loop unit step responses.

figure shows that the proposed methods give a better closed-loop response than the other methods.

## V. CONCLUSIONS

In this paper, a graph-based PID tuning technique is presented using the SBL and the weighted geometrical center (WGC) method. The principle of the technique is to first determine the two-dimensional stability regions in the parameter plane, then calculate the WGC points of these stable regions. Finally, considering these center points for the three-dimensional global stability region, the PID tuning parameters with the best time response are obtained. This WGC point can be used as a design preference for the PID controller because these parameters always ensure good time performance and guarantee closed-loop stabilization. Results indicate that system frequency response exhibits a satisfactory dynamical performance for WGC-based PID controller gains and the WGC method generates more attractive results as compared with other design approaches. One of the most important advantages of the proposed method is that it is applicable for all stable, unstable, and integrator time-delayed systems. Additionally, the proposed method is graph-based and quickly determines the optimum controller parameter values within the stability region resulting in good unit step response for time-delayed systems without using any optimization techniques.

**Peer-review:** Externally peer-reviewed.

**Author Contributions:** Concept – G.Ç., M.M.Ö., S.E.H.; Design – S.E.H.; Supervision – S.E.H.; Materials – G.Ç., M.M.Ö.; Data Collection and/or Processing – G.Ç., S.E.H.; Analysis and/or Interpretation – G.Ç., M.M.Ö., S.E.H.; Literature Review – G.Ç., M.M.Ö.; Writing – S.E.H.

**Declaration of Interests:** The authors have no conflicts of interest to declare.

**Funding:** The authors declared that this study has received no financial support.

## REFERENCES

- J. Zhu, T. Qi, D. Ma, and J. Chen, *Limits of Stability and Stabilization of Time-Delay Systems: A Small-Gain Approach*. Berlin: Springer, 2018.
- J. H. Park, T. H. Lee, Y. Liu, and J. Chen, *Dynamic Systems with Time-Delays: Stability and Control*. Berlin: Springer, 2019.
- K. Åström, and T. Hägglund, *Advanced PID Control*. ISA, 2006.
- A. O'Dwyer, *Handbook of PI and PID Controller Tuning Rules*. Imperial College Press, 2009.
- A. Visioli, "Fuzzy logic based tuning of PID controllers for plants with under-damped response," *IFAC Proc.*, vol. 33, no. 4, pp. 577–582, 2000. [\[CrossRef\]](#)
- V. A. Oliveira, L. V. Cossi, M. C. M. Teixeira, and A. M. F. Silva, "Synthesis of PID controllers for a class of time delay systems," *Automatica*, vol. 45, no. 7, pp. 1778–1782, 2009. [\[CrossRef\]](#)
- S. E. Hamamci, "A new PID tuning method based on transient response control," *Balkan J. Electr. Comput. Eng.*, vol. 2, no. 3, pp. 132–138, 2014. [\[CrossRef\]](#)
- Q. Wang, C. Lu, and W. Pan, "IMC PID controller tuning for stable and unstable processes with time delay," *Chem. Eng. Res. Des.*, vol. 105, pp. 120–129, 2016. [\[CrossRef\]](#)
- Z. Bingul, and O. Karahan, "Comparison of PID and FOPID controllers tuned by PSO and ABC algorithms for unstable and integrating systems with time delay," *Optimal Control Appl. Methods*, vol. 39, no. 4, pp. 1431–1450, 2018. [\[CrossRef\]](#)
- S. P. Bhattacharyya, A. Datta, and L. H. Keel, *Linear Control Theory: Structure, Robustness, and Optimization*. Boca Raton, United States of America: CRC press, 2009.
- N. Tan, and D. P. Atherton, "Design of stabilizing PI and PID controllers," *Int. J. Syst. Sci.*, vol. 37, no. 8, pp. 543–554, 2006. [\[CrossRef\]](#)

12. J. Ackermann, and D. Kaesbauer, "Design of robust PID controllers," in European Control. Conference, 522–527, 2001. [\[CrossRef\]](#)
13. N. Bajcinca, "Computation of stable regions in PID parameter space for time-delay systems," in IFAC Workshop on Time-Delay Systems, 23–28, 2005.
14. S. E. Hamamci, "An algorithm for stabilization of fractional-order time delay systems using fractional-order PID controllers," *IEEE Trans. Autom. Control*, vol. 52, no. 10, pp. 1964–1969, 2007. [\[CrossRef\]](#)
15. S. E. Hamamci, "PI and PID stabilization of neutral and retarded systems with time delay," *Turk. J. Electr. Eng. Comput. Sci.*, vol. 20(1), pp. 1189–1205, 2012. [\[CrossRef\]](#)
16. S. E. Hamamci, and N. Tan, "Design of PI controllers for achieving time and frequency domain specifications simultaneously," *ISA Trans.*, vol. 45, no. 4, pp. 529–543, 2006. [\[CrossRef\]](#)
17. M. A. Rahimian, and M. S. Tavazoei, "Application of stability region centroids in robust PI stabilization of a class of second-order systems," *Trans. Inst. Meas. Control*, vol. 34, no. 4, pp. 487–498, 2012. [\[CrossRef\]](#)
18. C. Onat, S. E. Hamamci, and S. Obuz, "A practical PI tuning approach for time delay systems," *IFAC Proc.*, vol. 45, no. 14, pp. 102–107, 2012. [\[CrossRef\]](#)
19. C. Onat, "A new concept on PI design for time delay systems: Weighted geometrical center," *Int. J. Innov. Comput. Inf. Control*, vol. 9, no. 4, pp. 1539–1556, 2013.
20. M. M. Ozyetkin, and N. Tan, "Practical tuning algorithm of PD<sup>l</sup> controller for processes with time delay," *IFAC PapersOnLine*, vol. 50, no. 1, pp. 9230–9235, 2017. [\[CrossRef\]](#)
21. M. M. Ozyetkin, C. Onat, and N. Tan, "PI-PD controller design for time delay systems via the weighted geometrical center method," *Asian J. Control*, vol. 22, no. 5, pp. 1811–1826, 2020. [\[CrossRef\]](#)
22. C. B. Kadu, S. Tidame, P. S. Vikhe, and S. M. Turkane, "Design of PI controller for liquid level system using Siemens distributed control system," *Int. J. Recent Technol. Eng.*, vol. 8, no. 3, pp. 2783–2789, 2019. [\[CrossRef\]](#)
23. M. M. Ozyetkin, C. Onat, and N. Tan, "PID tuning method for integrating processes having time delay and inverse response," *IFAC PapersOnLine*, vol. 51, no. 4, pp. 274–279, 2018. [\[CrossRef\]](#)
24. F. Schrödel, *Stability Region Based Robust Controller Synthesis*, PhD Thesis. Institute of Automatic Control, RWTH Aachen University, 2016. Aachen, Germany.
25. R. Toscano, "A simple robust PI/PID controller design via numerical optimization approach," *J. Process Control*, vol. 15, no. 1, pp. 81–88, 2005. [\[CrossRef\]](#)
26. Y. Lee, J. Lee, and S. Park, "PID controller tuning for integrating and unstable processes with time delay," *Chem. Eng. Sci.*, vol. 55, no. 17, pp. 3481–3493, 2000. [\[CrossRef\]](#)
27. C.-C. Chen, and H.-P. Huang, "Control-system synthesis for open-loop unstable process with time delay," *IEE Proc. Control Theor. Appl.*, vol. 144, no. 4, pp. 334–346, 1997. [\[CrossRef\]](#)
28. É. Poulin, and A. Pomerleau, "PID tuning for integrating and unstable processes," *IEE Proc. Control Theor. Appl.*, vol. 143, no. 5, pp. 429–435, 1996. [\[CrossRef\]](#)



Gülten Çetintaş received the B.S. and M.S. degree in Electrical and Electronics Engineering from Firat University, Elazığ, Turkey, in 2012 and 2016, respectively. She continues her PhD in Electrical and Electronics Engineering at Inonu University, Malatya, Turkey. She is currently working as a research assistant in the Department of Electrical and Electronics Engineering at Mus Alparslan University, Mus, Turkey. Her primary research interest lies in the area of systems and control.



Münevver Mine Özyetkin received the B.Sc. degree from Inonu University in Electrical and Electronics Engineering. She received the Ph.D. degree from Inonu University in Electrical and Electronics Engineering. She was awarded a grant by TUBITAK (The Scientific and Technological Research Council of Turkey) to conduct insulin control for diabetic patients between 2010 and 2011 in the USA. She is interested in fractional order control systems, design of fractional order controllers, robust control, and artificial pancreas.



Serdar Ethem Hamamcı received the B.S. degree in Electronics Engineering from Erciyes University in 1992 and the M.S. and PhD degrees in Electrical-Electronics Engineering from Firat University in 1997 and 2002, respectively. He is currently a full professor at Electrical-Electronics Engineering Department at Inonu University, Malatya, Turkey. His research interest includes control system design, fractional order systems, memristive systems, chaotic behaviors, electrical vehicles, and data mining.